The effect of Ni addition on microstructure and soft magnetic properties of FeCoZrBCu nanocrystalline alloys

Xingdu Fan, Yongtian Tang, Zhixiang Shi, Mufeng Jiang, and Baolong Shen

Citation: AIP Advances **7**, 056107 (2017); doi: 10.1063/1.4977229
View online: https://doi.org/10.1063/1.4977229
View Table of Contents: http://aip.scitation.org/toc/adv/7/5
Published by the American Institute of Physics

The effect of Ni addition on microstructure and soft magnetic properties of FeCoZrBCu nanocrystalline alloys

Xingdu Fan,[1,2] Yongtian Tang,[1] Zhixiang Shi,[2,a] Mufeng Jiang,[3] and Baolong Shen[1,a]

[1]*School of Materials Science and Engineering, Southeast University, Nanjing 211189, People's Republic of China*
[2]*Department of Physics, Southeast University, Nanjing 211189, People's Republic of China*
[3]*Londerful New Material Technology Corp., Nantong 226233, People's Republic of China*

(Presented 4 November 2016; received 23 September 2016; accepted 19 November 2016; published online 22 February 2017)

$(Fe_{0.7}Co_{0.3-x}Ni_x)_{88}Zr_7B_4Cu_1$ nanocrystalline alloys were developed with the aim of improving the magnetic properties while keeping high Curie temperature (T_C). It was revealed that Ni addition inhibited the precipitation of metastable *fcc*-(Fe,Co,Ni) phase hence increased thermal stability. Although the saturation magnetic flux density (B_s) showed a slight decrease, uniform nanostructure with small grain size and high volume fraction of crystals was formed with increasing Ni addition. As a result, the $(Fe_{0.7}Co_{0.3-x}Ni_x)_{88}Zr_7B_4Cu_1$ nanocrystalline alloys exhibited excellent magnetic properties with a high B_s of 1.54-1.79 T, low coercivity (H_c) of 17-20 A/m and low core loss of 9.1-11.1 W/kg at 1 T and 400 Hz. The combination of high T_C of 747-972 °C, low core loss as well as low material cost promised this FeCoNiZrBCu alloys broad application prospect at high temperature. [http://dx.doi.org/10.1063/1.4977229]

I. INTRODUCTION

The development of magnets for high temperature application requires new soft magnetic materials that possess (1) high magnetic flux density in small excitation magnetic field, (2) low residual magnetic induction (B_r), low coercivity (H_c) and core loss (P), (3) high stability of above properties at high temperature for a long time.[1–4] The traditional magnets have been unable to meet such requirements. Recently nanocrystalline soft magnetic alloys have attracted great attention due to their excellent soft magnetic properties and simple preparation. Nanocrystalline FeSiBNbCu,[5] FeZrBCu[6,7] and FeCoZrBCu[8] alloys patented under the trade name of FINEMET, NANOPERM and HITPERM are developed successively. Among them, FINEMET and NANOPERM alloys have good magnetic properties such as high effective permeability (μ_e), low H_c and core loss at room temperature. But due to the relative low Curie temperature (T_C) of both amorphous and nanocrystalline phase, the alloy can only be applied under 200 °C. On the other hand, HITPERM alloy exhibits high B_s, high T_C and good stability at high temperature. But the substitution of Co for Fe also leads to the increase of H_c and P because of large magneto-crystalline anisotropy constant (K_1) of Co element of 461×10^3 J/m^3.[9] Furthermore, the addition of Co also increases the material cost. Therefore, it is important to explore a nanocrystalline alloy with good soft magnetic properties, high T_C as well as low material cost.

It has been reported that the simultaneous Co and Ni addition favors the refinement of grain size.[10] Ni has a low K_1 of 5.7×10^3 J/m^3,[9] which is far lower than that of Fe and Co.

[a]Author to whom correspondence should be addressed. Electronic mail: zxshi@seu.edu.cn (Zhixiang Shi) blshen@seu.edu.cn (Baolong Shen)

The addition of Ni could help reduce effective magneto-crystalline anisotropy <K> thereby decreasing H_c and P. Therefore, FeCoNiZrBCu alloy is developed with the aim of improving soft magnetic properties. The $(Fe_{0.7}Co_{0.3})_{88}Zr_7B_4Cu_1$ is selected as the base alloy for the reason that first, the $(Fe_{0.7}Co_{0.3})$ alloy exhibits the highest B_s due to the strong exchange-coupling interaction between Fe and Co atoms on the basis of Slater-Pauling principle.[11,12] Second, lower Co content facilitates to reduce the material cost. As a result, nanocrystalline $(Fe_{0.7}Co_{0.3-x}Ni_x)_{88}Zr_7B_4Cu_1$ alloys were successfully prepared. The influence of Ni addition on crystallization behavior, microstructure and soft magnetic properties in FeCoNiZrBCu alloy system were investigated.

II. EXPERIMENTAL

Alloy ingots with nominal compositions of $(Fe_{0.7}Co_{0.3-x}Ni_x)_{88}Zr_7B_4Cu_1$ (x = 0, 0.1, 0.2, 0.3) were prepared by arc melting the mixtures of Fe (99.99 mass%), Co (99.99 mass%), Ni (99.99 mass%), Zr (99.99 mass%), B (99.5 mass%) and Cu (99.995 mass%) under a high purified argon atmosphere. Each ingot was melted five times to ensure compositional homogeneity. $(Fe_{0.7}Co_{0.3-x}Ni_x)_{88}Zr_7B_4Cu_1$ alloy ribbons were prepared by single roller melt spinning. The width and thickness of the ribbons were 1-2 mm and 25 μm, respectively. The melt-spun ribbons were annealed to develop nanocrystalline alloys. The annealing was carried out by keeping the ribbons in the tubular furnace preheated to annealing temperature (T_a) in vacuum atmosphere followed by water quenching cooling. Microstructures were identified by X-ray diffraction (XRD) with Cu $K\alpha 1$ radiation and transmission electron microscopy (TEM). Thermal stability was evaluated by differential scanning calorimeter (DSC) at a heating rate of 0.67 °C/s. B_s was measured with a vibrating sample magnetometer (VSM) under a maximum applied field of 800 kA/m and H_c was measured with a *DC* B-H curve tracer under a maximum applied field of 1 kA/m. The ribbons were wound into laminated toroids with 10 mm in outer diameter, 8 mm in inner diameter, subsequently isothermal annealed in the same condition with ribbons in order to determine the *AC* properties. Core losses were measured using an *AC* B-H analyzer.

III. RESULT AND DISCUSSION

According to the XRD results, the alloys with no or minor Ni addition (x = 0.1, 0.2) exhibit amorphous structure feature. While excessive Ni doping (x = 0.3) favors the precipitation of *bcc*-(Fe,Ni) phase hence decreases the glass forming ability. Figure 1 shows the DSC curves of $(Fe_{0.7}Co_{0.3-x}Ni_x)_{88}Zr_7B_4Cu_1$ melt-spun ribbons. The alloy with no Ni addition has four distinct exothermic peaks, demonstrating the crystallization process is complicated. But with Ni addition, the curves change to three exothermic peaks and the third crystallization peak has an obvious trend

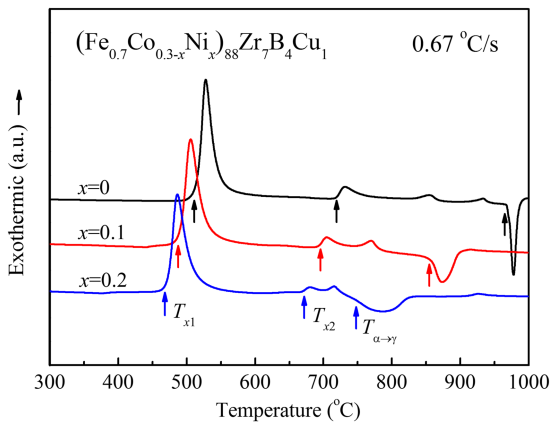

FIG. 1. DSC curves of $(Fe_{0.7}Co_{0.3-x}Ni_x)_{88}Zr_7B_4Cu_1$ melt-spun ribbons.

approaching the second one. Therefore, Ni addition effectively inhibits the precipitation of the second phases under high temperature leading to a more stable microstructure. The crystallization onset temperatures, denoted as T_{x1} and T_{x2} decrease monotonically with increasing Ni addition. Temperature differences (ΔT_x) between T_{x1} and T_{x2} have large value of more than 195 °C, reflecting the alloys exhibit good thermal stability, which is advantageous for annealing to obtain excellent soft magnetic properties. Meanwhile, the transition temperature of α phase to γ phase ($T_{\alpha\rightarrow\gamma}$) decreases from 972 °C for $x = 0$ to 747 °C for $x = 0.2$, respectively, suggesting that the transition temperature of *bcc*-(Fe,Co,Ni) from ferromagnetism to paramagnetism decreases, which is disadvantaged for high temperature application.

In order to analyze the crystallization behavior and microstructure, XRD measurement was carried out for $(Fe_{0.7}Co_{0.3-x}Ni_x)_{88}Zr_7B_4Cu_1$ alloy annealed at different temperatures. Figure 2 shows the XRD patterns of $(Fe_{0.7}Co_{0.2}Ni_{0.1})_{88}Zr_7B_4Cu_1$ alloy annealed at 380, 460, 540, 600 and 750 °C for 1 hour, respectively. The pattern of $(Fe_{0.7}Co_{0.3})_{88}Zr_7B_4Cu_1$ alloy annealed at 750 °C is also showed for comparison. As a result, a crystalline phase identified as *bcc*-(Fe,Co,Ni) phase superimposes on that of amorphous phase for $(Fe_{0.7}Co_{0.2}Ni_{0.1})_{88}Zr_7B_4Cu_1$ alloy annealed at 380 °C, which means the precipitation amount is small. As T_a increases, three characteristic diffraction peaks of *bcc*-(Fe,Co,Ni) phase can be detected. The average grain size (D) estimated by Scherrer's equation according to the (110) reflection peak is 15 and 12 nm for T_a = 460 and 540 °C, respectively. This phenomenon can be interpreted by the traditional nucleation mechanism,[13] which explains that forming fine nanostructure is determined by the nucleation rate and the growth rate.[14,15] The growth rate increases with increasing T_a while the nucleation rate has a maximum at an intermediate temperature. It is verified that the maximum nucleation rate may occur at 540 °C, where the highest number density of nanocrystals with smallest D is formed. Annealed at 600 °C produces a *bcc*-(Fe,Co,Ni) majority phase with a $Fe_{23}Zr_6$ minority phase. When annealed at 750 °C, a Fe_3Zr phase begins to precipitate due to the decomposition of $Fe_{23}Zr_6$ phase. As for the annealed $(Fe_{0.7}Co_{0.3})_{88}Zr_7B_4Cu_1$ alloy, in addition to the precipitation of *bcc*-(Fe,Co), $Fe_{23}Zr_6$ and Fe_3Zr phases, there is few amount of *fcc*-(Fe,Co) phase formed. Therefore, Ni addition inhibits the precipitation of metastable *fcc*-(Fe,Co) phase and increases the thermal stability, which is quite consistent with the DSC results.

In Fig. 3, the dependence of coercivity on annealing temperature for $(Fe_{0.7}Co_{0.3-x}Ni_x)_{88}Zr_7B_4Cu_1$ alloys is shown. It is seen that H_c has the same variation tendency toward T_a for $x = 0$ and 0.1. The annealed alloy at 380 °C exhibits obviously lower H_c compared to that of the as-quenched alloy due to the precipitation of *bcc*-(Fe,Co,(Ni)) phase. Then H_c increases gradually as T_a increases and reaches their maximum at 480 °C. As T_a continues to rise, nucleation rate increases, uniform nanostructure with small grain size is formed. According to the random anisotropy model proposed by Herzer,[16–18] which suggests that when grain size is smaller than exchange correlation length

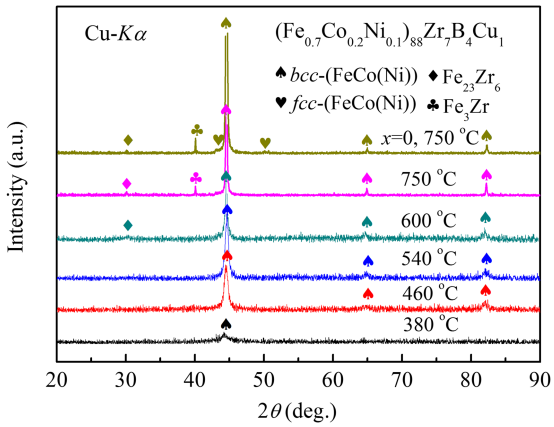

FIG. 2. XRD patterns of $(Fe_{0.7}Co_{0.2}Ni_{0.1})_{88}Zr_7B_4Cu_1$ alloy ribbons annealed at 380, 460, 540, 600 and 750 °C for 1 h, respectively. The pattern of $(Fe_{0.7}Co_{0.3})_{88}Zr_7B_4Cu_1$ alloy annealed at 750 °C for 1 h is showed for comparison.

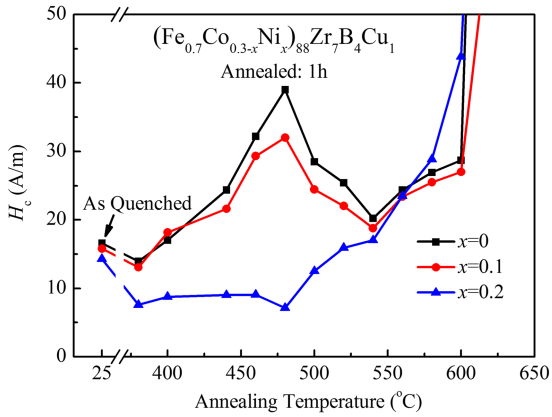

FIG. 3. The dependence of coercivity (H_c) on annealing temperature (T_a) for $(Fe_{0.7}Co_{0.3-x}Ni_x)_{88}Zr_7B_4Cu_1$ alloys.

($D << L_{ex}$), $<K>$ is essentially averaged out by exchange interaction. On the basis of relationship between H_c and $<K>$, H_c is a function of D and the rate of increase in H_c is almost proportional to D.[6] As a result, H_c decreases and reaches their minimum at 540 °C. After that, H_c increases again because of the growing grain size and takes drastic increase when T_a > 620 °C owing to the precipitation of second phase. The value of H_c for $(Fe_{0.7}Co_{0.1}Ni_{0.2})_{88}Zr_7B_4Cu_1$ alloy exhibits a similar variation. The difference is that the first increasing trend of H_c is much gentler while the minimum is got at a lower

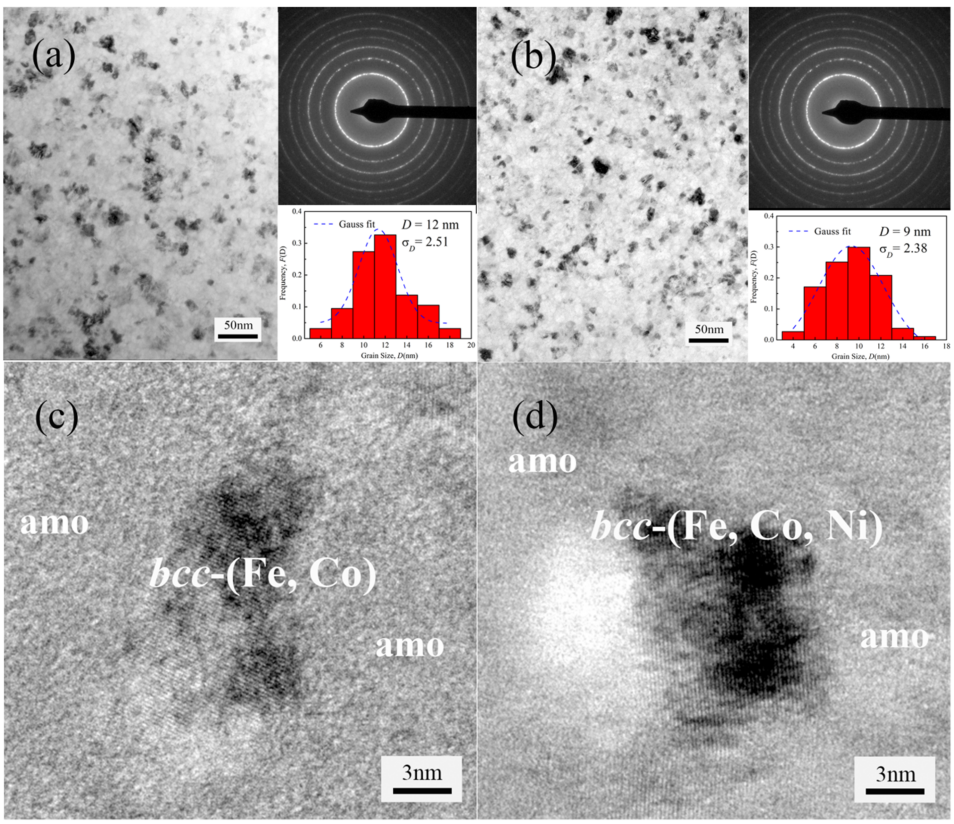

FIG. 4. The bright-field TEM images, selected area electron diffraction (SAED) patterns and grain size distributions of (a) $(Fe_{0.7}Co_{0.3})_{88}Zr_7B_4Cu_1$ and (b) $(Fe_{0.7}Co_{0.1}Ni_{0.2})_{88}Zr_7B_4Cu_1$ alloys annealed at 540 °C for 1 h, HRTEM images of (c) $(Fe_{0.7}Co_{0.3})_{88}Zr_7B_4Cu_1$ and (d) $(Fe_{0.7}Co_{0.1}Ni_{0.2})_{88}Zr_7B_4Cu_1$ nanocrystalline alloys.

temperature of 480 °C due to the low K_1 and low saturation magnetostriction (λ_s = -35×10^{-6}) of Ni element.[9,19]

Figure 4 shows the structure of $(Fe_{0.7}Co_{0.3-x}Ni_x)_{88}Zr_7B_4Cu_1$ (x = 0 and 0.2) alloys annealed at 540 °C for 1 h. The TEM images show that *bcc*-(Fe,Co) nanocrystalline grain precipitates from amorphous matrix after annealing. The statistic result reveals that grain distributes randomly from 6 to 18 nm with 12 nm in average for annealed $(Fe_{0.7}Co_{0.3})_{88}Zr_7B_4Cu_1$ alloy. But with Ni addition, the precipitated *bcc*-(Fe,Co,Ni) nanocrystalline grain is obviously smaller and the volume fraction of nanocrystals is much higher. Grain size distribution shows that nanocrystals mainly range in 6-12 nm. What is more, the average grain size is only 9 nm and the mean square deviation (σ_D) is 2.38, which is smaller than that of no Ni sample (σ_D = 2.51), reflecting a more uniform nanostructure.

The HRTEM observation reveals that the microstructure consists of residual amorphous phase and nanocrystalline *bcc*-phase that is embedded in amorphous matrix. The grains are both small with 10-12 nm in size. But the grain shapes have certain difference. The grain profile of $(Fe_{0.7}Co_{0.3})_{88}Zr_7B_4Cu_1$ nanocrystalline alloy is elongated while the $(Fe_{0.7}Co_{0.1}Ni_{0.2})_{88}Zr_7B_4Cu_1$ alloy appears circular, indicating the existence of orientation of grain growth in FeCoZrBCu alloy system, while Ni addition favors reducing the magneto-crystalline anisotropy, leading to the formation of spherical nanocrystals.

Figure 5 shows the dependence of core loss on frequency (f) for $(Fe_{0.7}Co_{0.3-x}Ni_x)_{88}Zr_7B_4Cu_1$ nanocrystalline alloys at maximum magnetic flux density (B_m) of 0.2 T, together with those of HITPERM alloy. Here the compared HITPERM alloy with composition of $(Fe_{0.5}Co_{0.5})_{88}Zr_7B_4Cu_1$ was prepared by melt-spun method followed by annealing at 560 °C for 1 h. The core loss of $(Fe_{0.7}Co_{0.3-x}Ni_x)_{88}Zr_7B_4Cu_1$ nanocrystalline alloys is smaller than that of HITPERM alloy over the whole frequency range. The value of P decreases with increasing Ni addition and takes obvious decrease at high frequency such as over 5 kHz.

Table I summarizes the magnetic properties of $(Fe_{0.7}Co_{0.3-x}Ni_x)_{88}Zr_7B_4Cu_1$ nanocrystalline alloys under several conditions compared with those of HITPERM alloy.[8,20] The substitution of Ni for Co results in a slight decrease in B_s because Ni element has only 2 unpaired electrons on 3d-track with the weakest magnetic moment (0.6 μB) compared with that of Fe (2.2 μB) and Co (1.6 μB),[21] which leads to the reduction in J_s. Meanwhile, Ni addition decreases the magneto-crystalline anisotropy and promotes the grain refinement. Therefore H_c decreases with the increase of Ni content. Low H_c also leads to low P. The value of $P_{10/400}$ and $P_{10/10k}$ for $(Fe_{0.7}Co_{0.1}Ni_{0.2})_{88}Zr_7B_4Cu_1$ nanocrystalline alloy is 9.1 W/kg and 465 W/kg, respectively, which is 50% less than that of $(Fe_{0.5}Co_{0.5})_{88}Zr_7B_4Cu_1$ nanocrystalline alloy. The combination of low H_c, low P and low material cost makes an outstanding economical application. Moreover, this alloys exhibit relatively high T_C of 747-972 °C, which promises their application at high temperature.

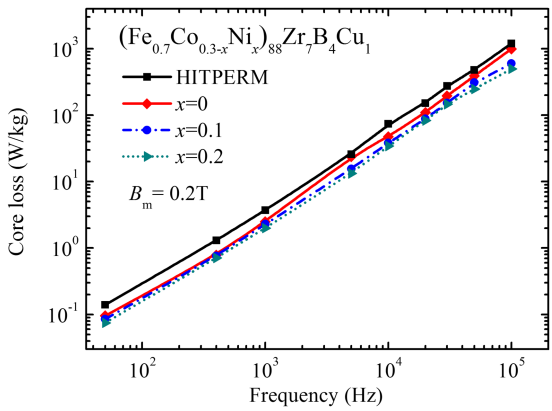

FIG. 5. The dependence of core loss (P) on frequency (f) for $(Fe_{0.7}Co_{0.3-x}Ni_x)_{88}Zr_7B_4Cu_1$ nanocrystalline alloys at maximum magnetic flux density (B_m) of 0.2 T, together with those of HITPERM alloy.

TABLE I. Magnetic properties of $(Fe_{0.7}Co_{0.3-x}Ni_x)_{88}Zr_7B_4Cu_1$ nanocrystalline alloys annealed at 540 °C for 1 h.[a]

Alloy	B_s (T)	H_c (A/m)	T_C (°C)	$P_{10/400}$ (W/kg)	$P_{10/10k}$ (W/kg)	$P_{2/20k}$ (W/kg)	$P_{2/100k}$ (W/kg)
$(Fe_{0.7}Co_{0.3})_{88}Zr_7B_4Cu_1$	1.79	20	972	11.1	813	110	993
$(Fe_{0.7}Co_{0.2}Ni_{0.1})_{88}Zr_7B_4Cu_1$	1.66	19	858	10.5	532	88	600
$(Fe_{0.7}Co_{0.1}Ni_{0.2})_{88}Zr_7B_4Cu_1$	1.54	17	747	9.1	465	83	498
HITPERM $(Fe_{0.5}Co_{0.5})_{88}Zr_7B_4Cu_1$ [8,20]	1.6-2.1	60	980	20	1000	-	-

[a]The symbols $P_{10/400}$, $P_{10/10k}$, $P_{2/20k}$ and $P_{2/100k}$ stand for core loss at 1 T at 400 Hz and 10 kHz, and at 0.2 T at 20 kHz and 100 kHz, respectively.

IV. CONCLUSION

In conclusion, the effect of Ni addition on crystallization behavior, microstructure and soft magnetic properties in $(Fe_{0.7}Co_{0.3-x}Ni_x)_{88}Zr_7B_4Cu_1$ alloy system was investigated. The results show that the substitution of Ni for Co increases the thermal stability, reduces the magneto-crystalline anisotropy hence leading to the ultrafine nanostructure. The $(Fe_{0.7}Co_{0.3-x}Ni_x)_{88}Zr_7B_4Cu_1$ alloys annealed at 540 °C for 1 h exhibit a high B_s of 1.54-1.79 T, low H_c of 17-20 A/m and low core loss of 9.1-11.1 W/kg at 1 T and 400 Hz, respectively, which is obviously superior to the $(Fe_{0.5}Co_{0.5})_{88}Zr_7B_4Cu_1$ nanocrystalline alloy.

ACKNOWLEDGMENTS

This work was supported by the National Natural Science Foundation of China (Grant Nos. 51401052 and 51471050), Key Program of National Natural Science Foundation of China (Grant No. 51631003), the National Key Research and Development Program of China (Grant No. 2016YFB0300500) and Jiangsu Planned Projects for Postdoctoral Research Funds (Grant No. 1302044B).

[1] M. E. McHenry, M. A. Willard, and D. E. Laughlin, Prog. Mater. Sci. **44**, 291 (1999).
[2] M. E. McHenry and D. E. Laughlin, Acta Mater. **48**, 223 (2000).
[3] Y. Yoshizawa, Scripta Mater. **44**, 1321 (2001).
[4] K. E. Knipling, M. Daniil, and M. A. Willard, Appl. Phys. Lett. **95**, 222516–3 (2009).
[5] Y. Yoshizawa, S. Oguma, and K. Yamauchi, J. Appl. Phys. **64**, 6044 (1988).
[6] K. Suzuki, A. Makino, N. Kataoka, A. Inoue, and T. Masumoto, Mater. Trans., JIM **32**, 93 (1991).
[7] K. Suzuki, A. Makino, A. Inoue, and T. Masumoto, J. Appl. Phys. **70**, 6232 (1991).
[8] M. A. Willard, D. E. Laughlin, and M. E. McHenry, J. Appl. Phys. **84**, 6773 (1998).
[9] S. Chikazumi, *Physics of Ferromagnetism* (Oxford Sci. Pub., 2009).
[10] K. E. Knipling, M. Daniil, and M. A. Willard, J. Appl. Phys. **117**, 172611 (2015).
[11] J. C. Slater, J. Appl. Phys. **8**, 385 (1937).
[12] L. Pauling, Phys. Rev. **54**, 899 (1938).
[13] H. Hermann, N. Mattern, S. Roth, and P. Uebele, Phys. Rev. B. **56**, 13888 (1997).
[14] W. M. Yang, H. S. Liu, C. C. Dun, Y. C. Zhao, and L. M. Dou, Mater. Sci. Technol. **28**, 1465–1469 (2012).
[15] L. Xue, H. S. Liu, L. T. Dou, W. M. Yang, C. T. Chang, A. Inoue, X. M. Wang, R. W. Li, and B. L. Shen, Mater. Design. **56**, 227 (2014).
[16] G. Herzer, IEEE Trans. Magn. **26**, 1397 (1990).
[17] G. Herzer, Journal of Magn. Magn. Mater. **112**, 258 (1992).
[18] G. Hezer, Acta Mater. **67**, 718 (2013).
[19] A. E. Clark and H. S. Belson, Phys. Rev. B **5**, 3642 (1972).
[20] M. A. Willard and M. Daniil, *Nanoscale Magnetic Materials and Applications*(Springer Pub., 2009), Chap. 13, 373.
[21] K. Yamauchi and T. Mizoguchi, J. Phys. Soc. Jpn. **39**, 541 (1975).